# Effect of Processing Conditions on the Structure and Properties of Polypropylene Spunbond Fabrics

**Rammohan Nanjundappa,* Gajanan S. Bhat**

*Department of Materials Science and Engineering, The University of Tennessee, Knoxville, Tennessee 37996-2200*

Received 15 February 2005; accepted 29 April 2005
DOI 10.1002/app.22148
Published online in Wiley InterScience (www.interscience.wiley.com).

**ABSTRACT:** The structure and properties of a spunbond fabric are determined by numerous process variables. The development of fiber morphology is influenced and controlled by extrusion and quenching conditions. The properties of the fabric are the result of the properties of the filaments, their arrangement in the web, and the bonding conditions. It is therefore critical to understand the relationship between the process conditions and the properties of the fabrics produced. This study was conducted to investigate the effects of some of the important process variables on the structure and properties of the filaments and ultimately on that of the fabrics. Process variables such as polymer throughput rate, cooling and suction air speed, web basis weight, and bonding temperature were investigated. Filament samples were collected before bonding and were analyzed for various properties such as crystallinity, crystallite size, birefringence, density, thermomechanical stability, and tensile properties. The fabric samples were analyzed for tensile properties, tear strength, stiffness, and crystallinity. Ruptured strips obtained from the tensile test were observed with a scanning electron microscope to understand the failure mechanism. The results were statistically analyzed to evaluate the effect of process variables on the properties and to predict the properties for different process conditions. The findings are helpful in determining the optimum processing conditions so as to achieve the desired properties.
 J Appl Polym Sci 98: 2355–2364, 2005

**Key words:** spunbonding; polypropylene; nonwovens; thermal bonding; crystallinity; tensile properties; failure mechanism

## INTRODUCTION

Spunbonding is one of the most widely used methods of producing nonwovens. It is based on the melt-spinning technique and has many similarities to it.[1,2] The molten polymer is forced through a block of spinnerets to produce a curtain of filaments (Scheme 1). The air ducts force air through the spinning chamber at high speed, the filaments are drawn by the air drag and also continuously cooled. The drawn filaments then pass through a venturi, which is a high-velocity-low-pressure zone and a distributing chamber. This causes the filaments to fan out and randomize, which are then laid on a moving collector belt. Suction fans below the porous belt remove the air from the filaments and help in the lay-down. The random web of filaments is then strengthened by bonding. Thermal point bonding is mostly employed for webs of low to medium basis weight

The entire process is a continuous one and hence, changes in process variables are complex to the extent that, changing one necessitates other process changes. Earlier studies showed that decrease in throughput and primary air temperature led to decrease in filament diameter, accompanied by increase in crystallinity, birefringence, tensile strength, initial modulus, thermal stability, and density.[3–5] Thermal bonding of the filaments is an inherent part of the process and is affected by the varying spinning conditions. Bonding conditions will have to be modified to accommodate different conditions of spinning. For example, increasing the rate of polymer throughput when producing a fabric with a certain basis weight necessitates an increased line speed. The change in throughput causes change in filament diameter, quench rate, internal morphology, and lay-down pattern. Higher line speed reduces the time of contact in the nip of the bonding rollers. The choice of bonding conditions will have to consider these factors so as to produce a fabric with optimum properties.[6–9]

The objective of this research was to (1) study the relation between filament and fabric properties, (2) study the changes in filament morphology on thermal bonding, (3) study the mechanism of rupture of the fabric as related to the filament properties and process changes, and (4) predict the optimum process conditions to achieve the best fabric properties.

Various tests were conducted on the unbonded filaments and the bonded fabrics to achieve the objectives. The rupture mechanism was observed with a

**Present address:* Colbond Nonwovens, Sand Hill Road, P. O. Box 1057, Enka, NC 28728.
*Correspondence to:* G. S. Bhat (gbhat@utk.edu).

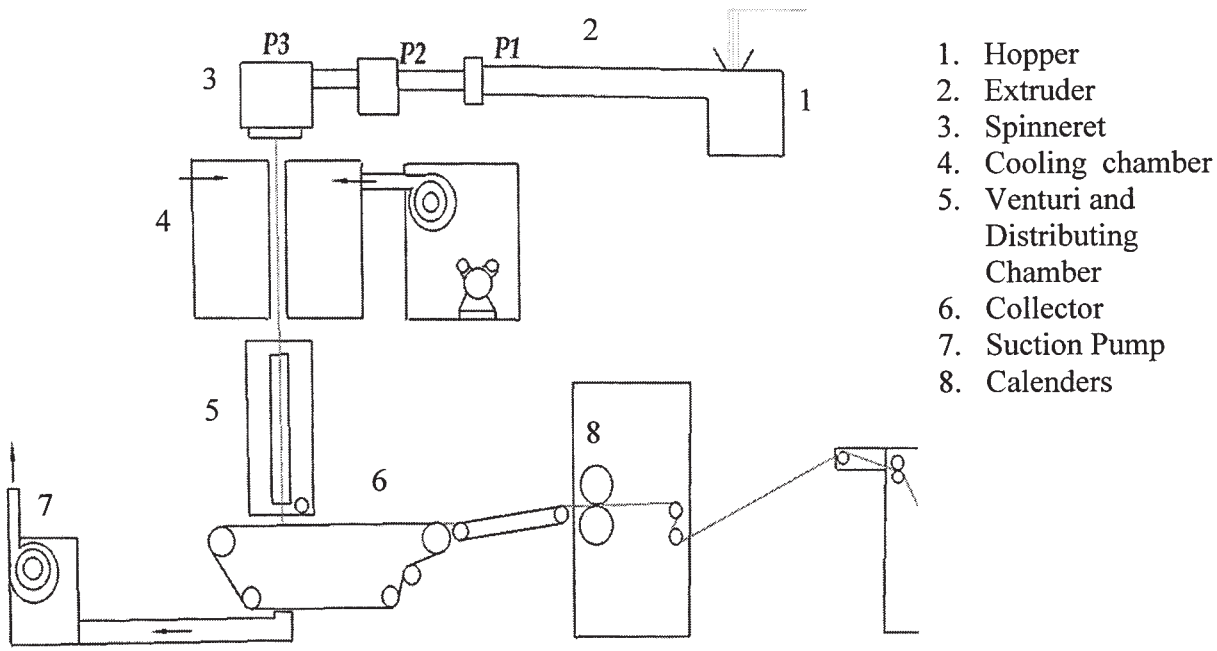


**Scheme 1** Schematic diagram of the Reicofil spunbonding line.

scanning electron microscope. The results were statistically analyzed to predict the properties.

## EXPERIMENTAL

### Processing

Processing was done at the Textiles and Nonwovens Development center (TANDEC) of the University of Tennessee, Knoxville, using the modified Reicofil®I spunbond line. Polypropylene polymer with a melt flow rate of 35 (PP3155), supplied by ExxonMobil Chemical Company was used. The samples were produced with three process variables namely: polymer throughput rate, web basis weight, and bonding temperature. Each variable was increased in four steps as shown in Scheme 2, to encompass a broad range of process conditions. Low basis weights (17 g/m$^2$) were not produced at the higher throughputs (0.35, 0.43 g/hole/min) because of the speed limitation of the collector belt. Other process conditions for each sample were chosen based on suggestions by the machine manufacturer. Airflow was increased with increase in throughput, and calender pressure was increased with increase in basis weight. The bonding consisted of point bonding system with a smooth bottom roll, and an embossed top roll with diamond pattern and ~15% contact area.

### Characterization

Filament diameter and filament bundle orientation were measured employing the WEBPRO® image anal-

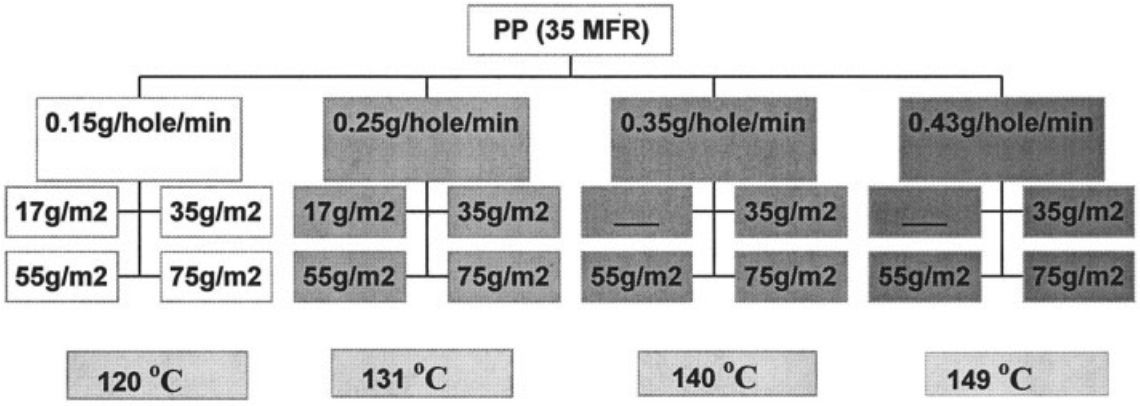


**Scheme 2** Schematic of process variables.

**TABLE I**
**Properties of the Filament before Bonding**

| Throughput (g/hole/min) | Filament diameter ($10^{-6}$ m) | Crystallinity by DSC (%) | Crystallite size (Å) | Birefringence ($10^{-3}$) | Peak stress (g/tex)[a] | Peak extension (%)[a] |
|---|---|---|---|---|---|---|
| 0.15 | 19.3 | 42.3 | 43 | 16.6 | 21.3 (13.4) | 376 (14.0) |
| 0.25 | 17.4 | 43.6 | 65 | 22.3 | 24.0 (19.1) | 312 (13.1) |
| 0.35 | 17.7 | 43.6 | 66 | 23.0 | 23.7 (16.7) | 297 (13.9) |
| 0.43 | 18.4 | 43.9 | 86 | 22.0 | 25.2 (12.6) | 296 (13.1) |

[a] Percentage coefficients of variations are given in parenthesis.

ysis software.[10,11] One hundred samples were taken for diameter and 50 samples for orientation. Birefringence was computed by the retardation technique using an optical microscope with a compensator. An average of 30 readings was taken. Crystallinity was measured using the Mettler DSC25, and an average of five scans was used. All samples were scanned at a heating rate of 10°C/min in nitrogen purge. Crystallinity was calculated using a $\Delta H$ value of 190 J/g for 100% crystalline polypropylene. Thermo-mechanical analysis (TMA) was carried out using the Mettler TMA 40. A scanning rate of 10°C/min was used and measurements were made at a tension of 0.05 N.

Wide-angle X-ray diffraction studies were done using the Rigaku Geigerflex Diffractometer. The Phillips flat plate X-ray diffractometer was employed to obtain X-ray photographs. Samples were prepared with the filaments parallel on a sample holder. The sample was exposed to X-rays of wavelength 1.54183 Å, with an exposure time of 6 h. Crystal size was calculated using the Scherrer equation from the measured full width half maximum intensity of the reflection peaks in the equatorial scans.[12] Equatorial scans were obtained from $2\theta = 10°–30°$ in steps of 0.01° and a dwell time of 4 s. Duco cement was used as glue for sample preparation for equatorial scans. Use of Duco cement was helpful in sample preparation from only bond areas and very short fibers from unbonded regions of the web. Duco cement is totally amorphous and does not interfere with crystalline peaks of polypropylene. The Rigaku WAXD system was operated at 35 kV and 30 mA. Bonded and unbonded regions were carefully separated from the web, using a pair of sharp scissors and analyzed for crystal size.

Tensile testing of the filaments was done with a bundle of five filaments at a gauge length of 5.08 cm and a cross-head speed of 5.08 cm/min, using a United tensile tester. Fabric samples were tested along machine and cross machine directions with a gauge length of 12.7 cm and a cross-head speed of 12.7 cm/min.

Scanning electron microscopy provided the pictures for the analysis of the mechanism of rupture. The Hitachi *S*-3000N environmental microscope was used with the back-scattered electron detector. A small volume of air in the specimen chamber neutralized charging by ionizing and being attracted to the charged sites. The ruptured samples were observed from the point of clamping toward the point of break. Images were recorded noting the increasing deformation of the structure as the point of rupture was approached.

Statistical analysis, a useful tool in predicting the optimum process conditions,[13,14] was carried out on the tensile results, using the SAS® software. The RSREG regression procedure was employed to fit a response surface to the actual data set. The regression equation, $R^2$-value, and significance of the results were also computed.

## RESULTS AND DISCUSSION

### Filament properties

The properties of the unbonded filament samples collected before bonding are shown in Table I. The diameters of the filaments produced with increasing throughputs are in the same range. Hence, there is an increasingly higher draw force with increase in throughput, which was accomplished by adjusting the air rate for each throughput. Maintaining the diameter same is important in comparing the data by avoiding another variable. However, the higher draw ratio leads to different stages of development of filament morphology. It causes an increase in strength and reduction in extension of the filaments by changing the molecular orientation, as a result of the drawing stress. This is accompanied by higher crystallinity as well as larger crystallite sizes. Consequently, the filament becomes thermomechanically more stable, as it can be interpreted from Figure 1. This is a result of higher molecular orientation, crystallinity, and larger crystallite size. Flat plate X-ray photographs show increasing crystallinity and crystalline orientation with increasing throughput. This is characterized by the increasing intensity of the arcs and the arcs becoming sharper (Fig. 2).

### Fabric properties

The fabric properties are influenced by the properties of the filaments shown earlier and other variables in

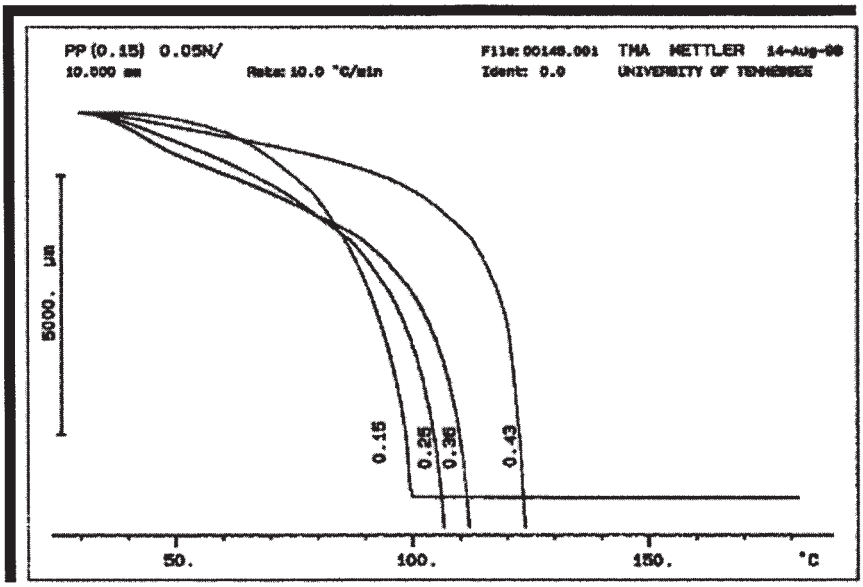


**Figure 1** TMA scans of filaments produced at different melt throughputs.

the process after the formation of the filaments, which influence the properties of the filaments exposed to heat in calender. The lay down of the filaments on the conveyor belt is affected by the air speed in the distributing chamber and the belt speed that is governed by the throughput rate and the basis weight. The belt speed affects the calendering time, and the calender itself has calender surface temperature and nip pressure as the variables.

Increasing the basis weight, maintaining the polymer throughput rate constant, requires the line speed to be lower and hence decreases the tendency for the filaments to be oriented in the direction of motion. This is seen as the ratio of filament bundles along MD to CD reducing and reaching a value close to 1. The same trend is seen for all the throughputs, as shown in Figure 3. Increasing throughput with basis weight constant is a more complex matter. Since, we have established that the filament diameters are essentially the same for all the throughputs, we have higher draw ratios to a certain extent, compensating for the higher line speed. It is further complicated by higher air speeds for higher throughputs. The trend for MD/CD orientation is not very evident, as seen from the data in Figure 3.

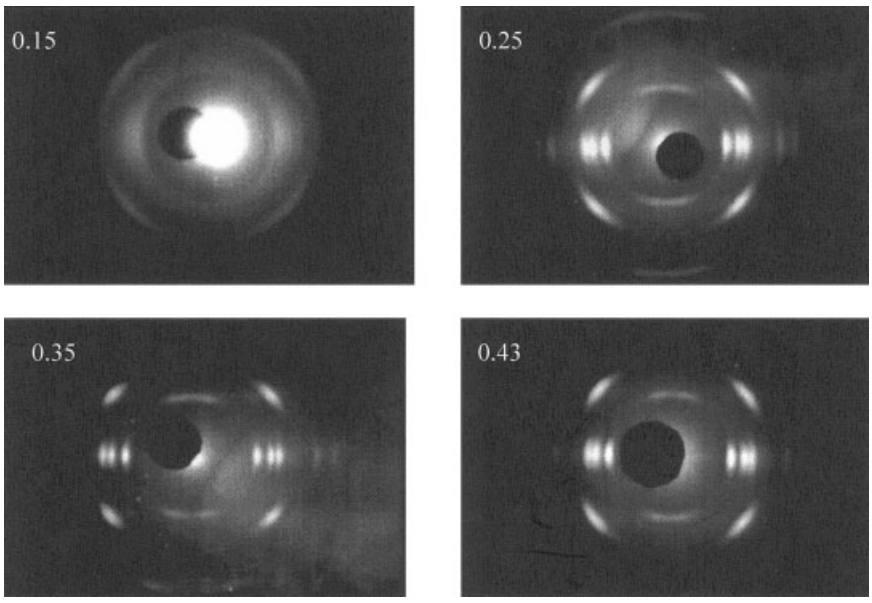


**Figure 2** WAXD photographs of filament samples produced at different throughput (as indicated).

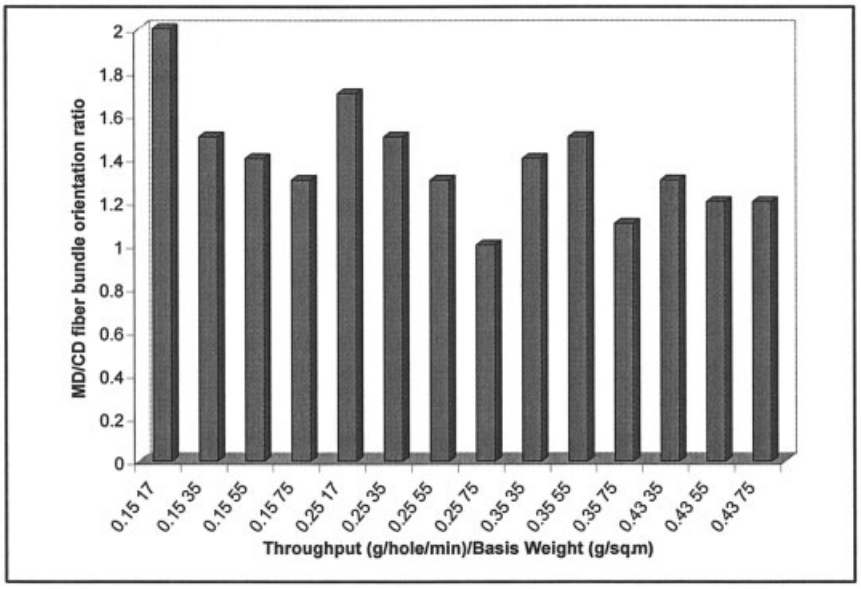


**Figure 3** Fiber bundle orientation with increasing basis weight and throughput.

The tensile properties of the fabric are affected by the orientation, the filament properties, and the bonding conditions. The bonding conditions including calender temperature, calender pressure, and contact time seem to have the greatest effect on the tensile properties. As shown in Figure 4, when bonding temperature is increased, with throughput and basis weight constant, it is seen that peak stress increases, reaches a peak value, and then declines. The same trend is seen for peak extension as well. The main contributor to this trend is the manner in which the filaments bond together in the area of the bond. This factor is discussed in detail in the next section. There is an increase in crystallinity and crystallite sizes in the unbonded and bonded areas of the fabric, but, differences in crystal sizes between samples bonded at dif-

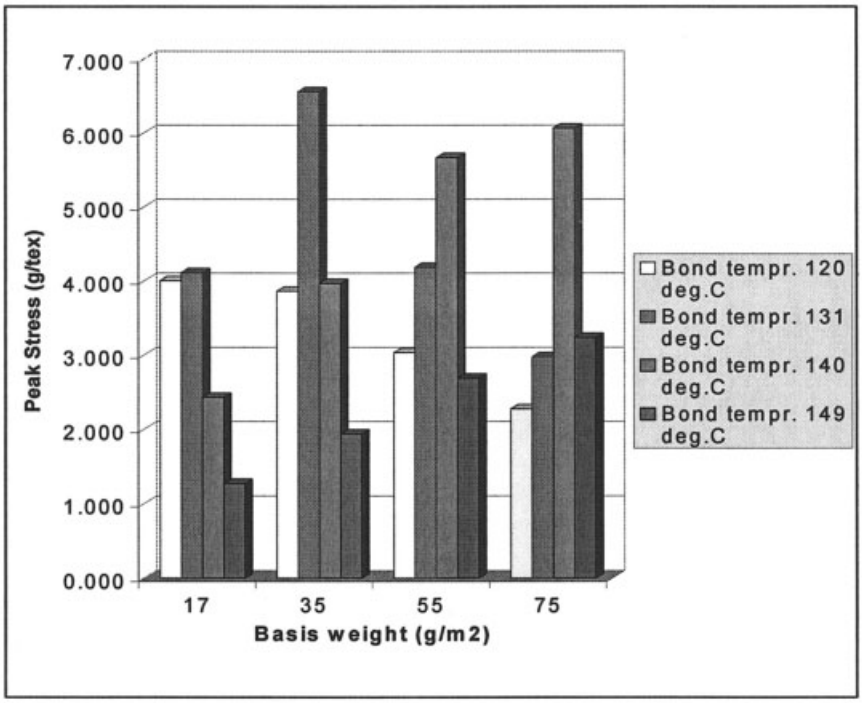


**Figure 4** Peak stress with increasing basis weight and bonding temperature at throughput 0.15 g/hole/min tested along the machine direction.

**TABLE II**
**Crystalline Sizes and Crystallinity of Selected Fabrics**

| Bonding temperature (°C) | Crystallite size (Å) | | Crystallinity (%) | |
|---|---|---|---|---|
| | Unbonded area of fabric | Bonded area of fabric | Unbonded area of fabric | Bonded area of fabric |
| 120 | 121 | 164 | 41.6 | 46.0 |
| 131 | 120 | 168 | 43.6 | 47.4 |
| 140 | 135 | 169 | 43.8 | 47.3 |
| 149 | 114 | 169 | 42.1 | 47.4 |

All samples with throughput 0.35 g/hol/min and basis weight 35 g/m$^2$ are bonded at increasing bonding temperatures.

ferent bonding temperatures are minimal (Table II). The effect of contact time becomes important when throughput is increased with fabric weight and bonding temperature is kept constant, as it can be interpreted from Figure 5. Increase in throughput requires increased bond temperature to attain optimum transfer of heat and to produce a fabric with optimum properties. Finally, increasing basis weight also requires higher bonding temperatures along with higher bonding nip pressure to attain optimum properties.

### Mechanism of rupture

Observation of the bond areas with the help of a scanning electron microscope yielded important information about the nature of bonding between filaments. The effect of throughput (less contact time) and bonding temperature seem to have an overriding effect on the differences in filament properties in determining the nature of the bond. As seen from Figure 6, with increase in bonding temperature, maintaining throughput and basis weight constant, the filaments in the bond area gradually lose their round shape and become flattened. This leads to a greater surface area of the filament participating in the bond to make it more coherent. A similar effect is seen with reduction in polymer throughput. Reducing throughput increases the contact time in the calender nip and causes the filaments to flatten out. Reducing throughput also reduces the fiber morphology development, which may have an effect on the shape of the filaments and the extent of bonding. The effect of fiber morphology on bonding showing similar results has been observed before.[6]

Considering the extremes of samples bonded at low bonding temperatures or high throughput, both of which have similar bond areas as explained earlier, the mode of rupture proceeds by disintegration of the bond area. As higher stress is encountered, filaments peel off from the bond until the entire bond disappears, as seen in Figure 7. Final rupture takes place when these filaments break. These samples characteristically exhibit low peak stress and high breaking strains.

The other extreme is the samples bonded at high bonding temperatures or low throughput. In this case, the bond areas are strong because of larger areas of bonding in the individual filaments. The higher temperatures or higher contact times that produce such bonds also cause the bond peripheries to be weaker. The bond periphery, in this case, will be expected to have polymer that is squeezed out of the bond by the lands of the calender, which would have solidified

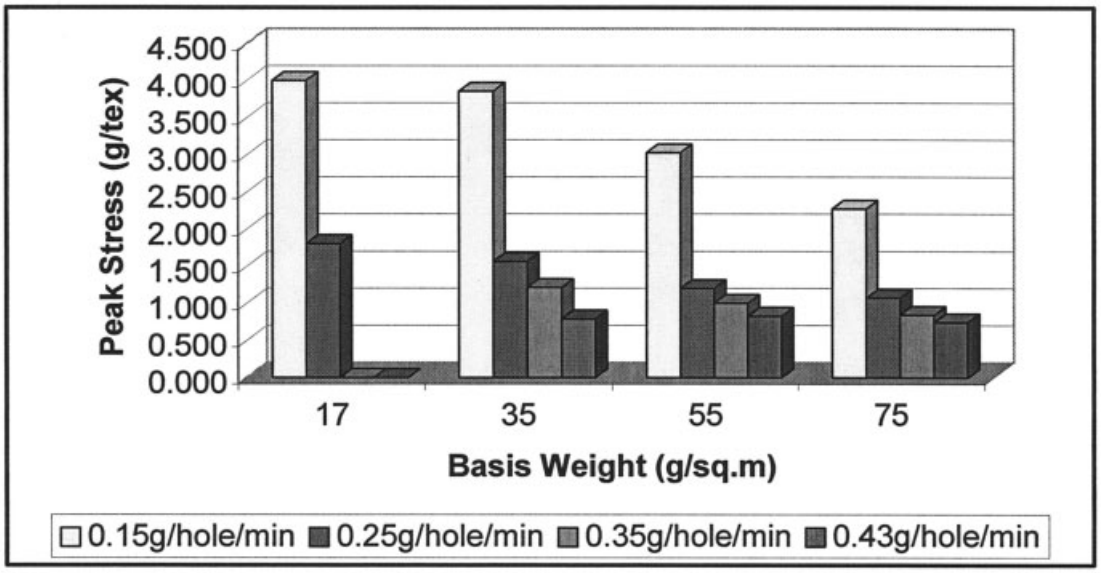


**Figure 5** Peak stress with increasing throughput and fabric weight at bond temperature 120°C tested along the machine direction.

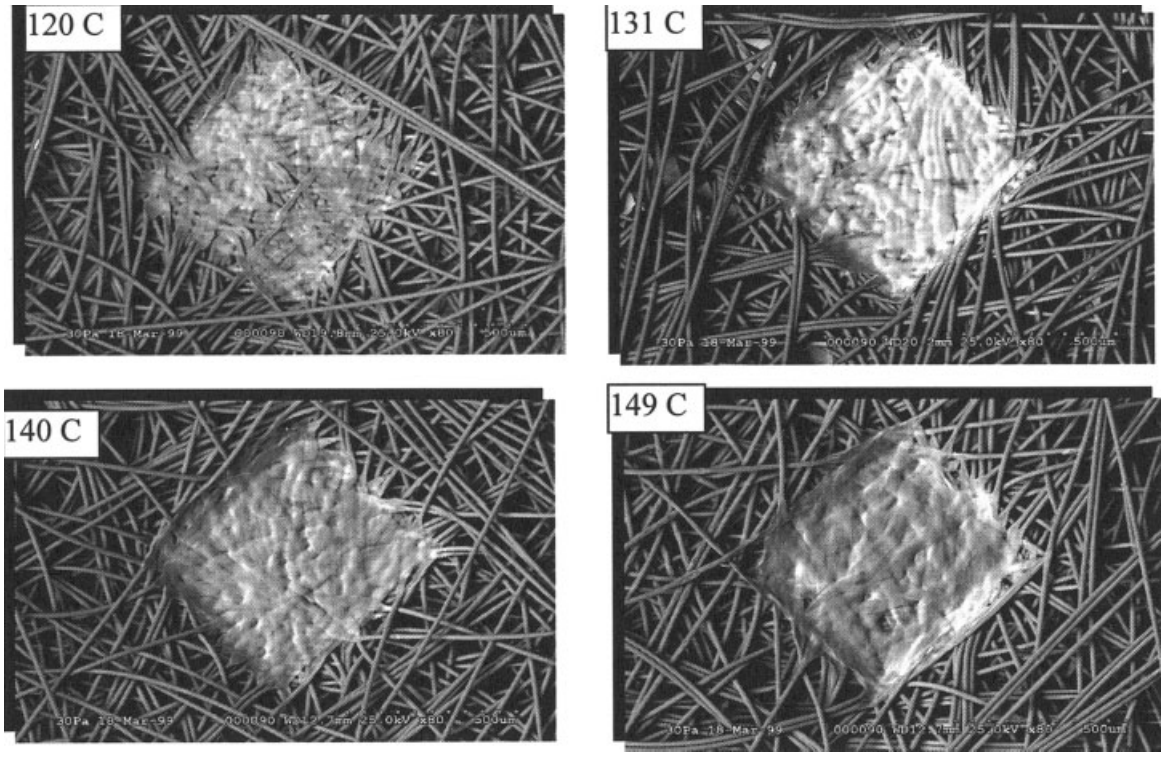


**Figure 6** Bond structure of spunbonded webs bonded at different temperatures (120, 131, 140, and 149°C).

under conditions of no tension. This area ruptures first, as seen in Figure 8.

The optimum tensile property sample ruptures due to filament separation from the bond areas, but the bond itself is deformed and bond disintegration occurs at a higher stress level than in the sample bonded at low bonding temperature. Some points of rupture also occur at the bond periphery (Fig. 9). Because of the combination of stronger bonding and extension of the bonds, the sample exhibits the highest breaking load (Fig. 10).

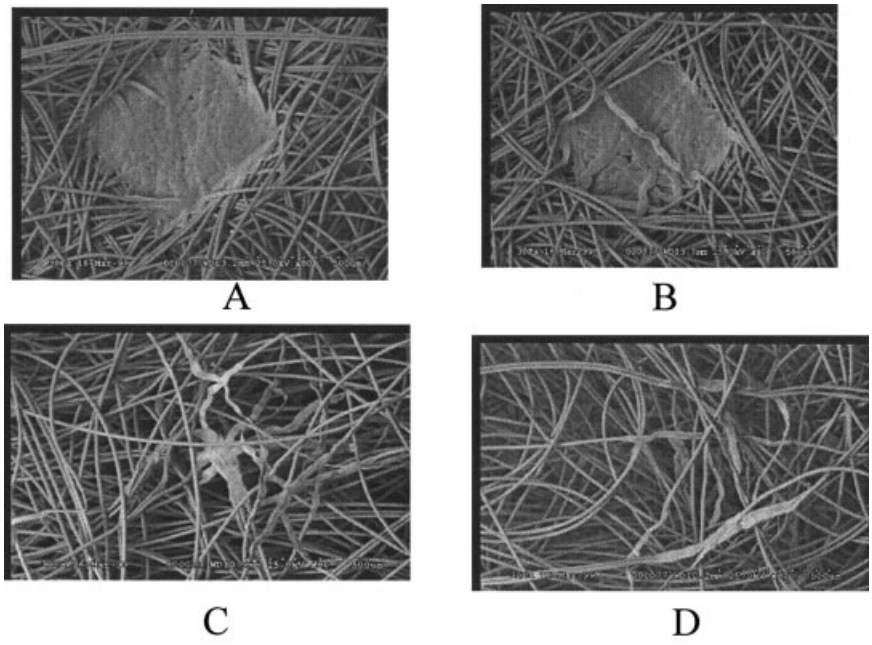


**Figure 7** Failure mechanism of samples bonded at a lower temperature (120°C): before testing (A); in the beginning of tensile deformation (B); close to failure (C); and at/after failure (D).

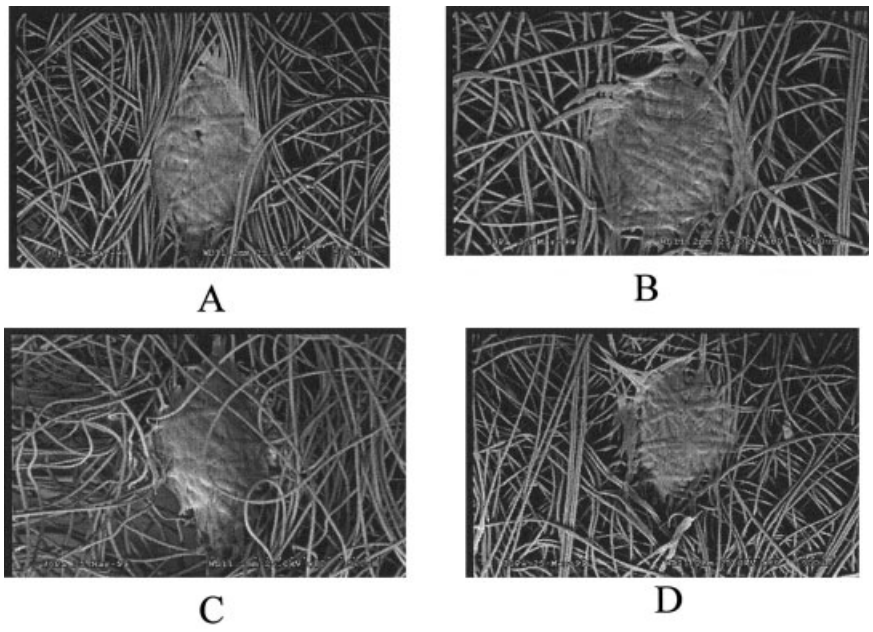


**Figure 8** Failure mechanism of samples bonded at a higher temperature (149°C): before testing (A); in the beginning of tensile deformation (B); close to failure (C); and at/after failure (D).

**Statistical analysis**

Statistical analysis showed that all the three process variables have a significant effect on the fabric tensile properties. Response surfaces were fitted using the least-squares method to predict the response variables peak stress, peak extension, and breaking energy. The $R^2$-value showed moderate to good fit to the original data. Figure 11 shows the predicted response surface at a throughput of 0.35 g/hole/min at all basis weights and bonding temperatures. The $R^2$-value was 0.9118. Observation of the graph and analysis shows that bonding temperature has

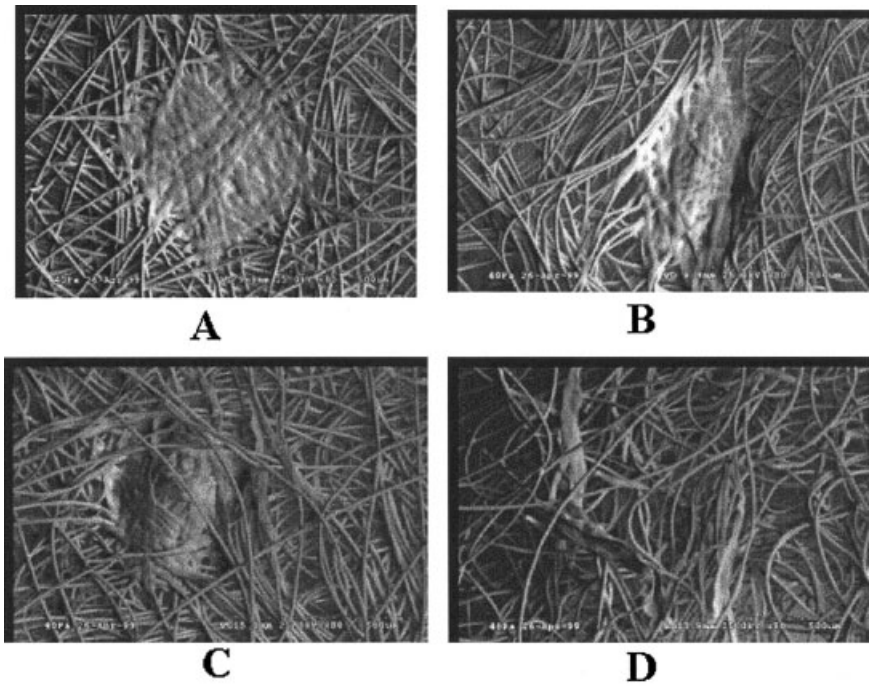


**Figure 9** Failure mechanism of samples bonded at an optimum temperature (140°C): before testing (A); in the beginning of tensile deformation (B); close to failure (C); and at/after failure (D).

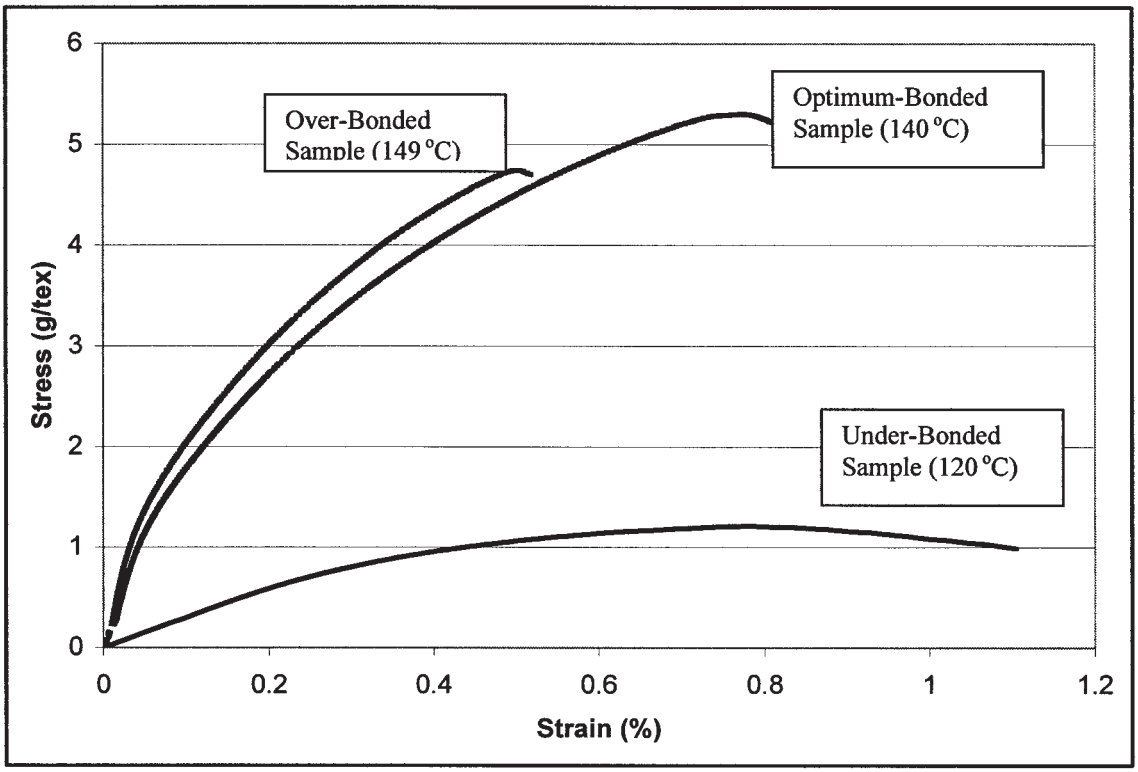


**Figure 10** Stress–strain curves for samples analyzed for mechanism of rupture.

the major contribution to the response surface than that of basis weight.

## CONCLUSIONS

A broad range of process variables were studied to investigate the relation between process and properties. It was observed that changing process conditions considerably affect the morphology and properties of the filaments. Also, the structure of the filaments changes during the course of bonding. Hence, the final structure is the net result of the spinning conditions and the bonding conditions. The optimum process conditions to produce a fabric with the best properties have been determined for a 35 MFR polypropylene polymer. Statistical analysis showed that bonding conditions such as temperature had a major effect on tensile properties, and helped in predicting the properties for a given set of conditions, with good confidence. The analysis of the mode of rupture helps

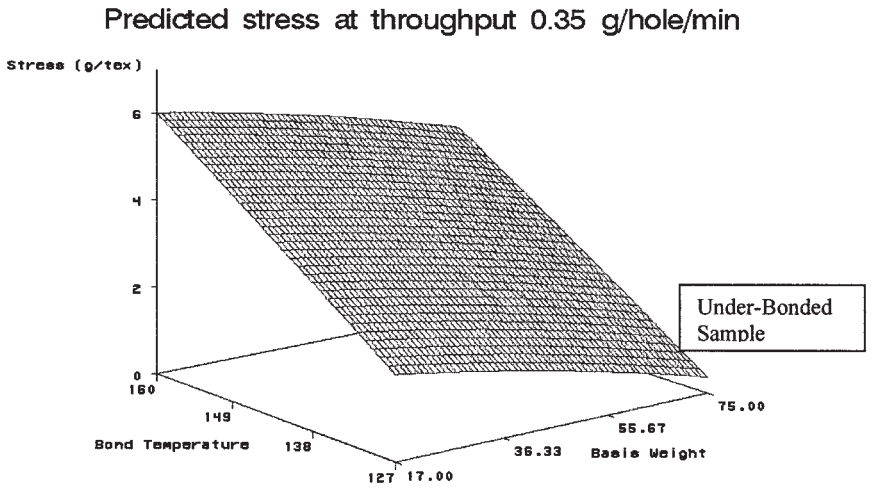


**Figure 11** Predicted response surface for peak stress at throughput 0.35 g/hole/min with all four basis weights and bonding temperatures.

understand the translation of change of process conditions into changes in fabric tensile properties. It was clearly shown that failure mechanisms are different for under-bonded, over-bonded, and optimum-bonded fabrics. By selecting appropriate bonding conditions based on fiber morphology and basis weight, it should be possible to produce fabrics with the desired tensile properties.

The authors thank ExxonMobil Chemical Company for providing the polymer and supporting the spunbond facilities at UTK, that were used in this research. Help from Gary Wynn, Jack Wyrick, and Anthony Whaley in processing and partial financial support from the center for materials processing (CMP) at UTK are acknowledged.

## References

1. Bhat, G. S.; Malkan, S. R. J Appl Polym Sci 2002, 83, 572.
2. Malkan, S. R.; Wadsworth, L. C.; Davey, C. Int Nonwovens J 1992, 2, 42.
3. Zhang, D.; Bhat, G. S.; Malkan, S. R.; Wadsworth, L. C. Text Res J 1998, 68, 27.
4. Zhang, D.; Bhat, G. S.; Malkan, S. R.; Wadsworth, L. C. J Therm Anal 1997, 49, 161.
5. Bhat, G. S.; Zhang, D.; Malkan, S. R.; Wadsworth, L. C. In Proceedings of the 4th Annual TANDEC Conference, Knoxville, TN, 1994; Nov 14–16.
6. Chand, S.; Bhat, G. S.; Spruiell, J. E.; Malkan, S. R. Int Nonwovens J 2002, 11, 12.
7. Bhat, G. S.; Jangala, P.; Spruiell, J. E. J Appl Polym Sci 2004, 92, 3593.
8. Chand, S.; Bhat, G. S.; Spruiell, J. E.; Malkan, S. R. Thermochim Acta 2001, 367–368, 155.
9. Dharmadhikary, R. K.; Gilmore, T. F.; Davis, H. A.; Batra, S. K. Text Prog 1995, 26, 1.
10. Huang, X.; Bresee, R. R. INDA J Nonwovens Res 5, 1993, 3, 28.
11. Huang, X.; Bresee, R. R. INDA J Nonwovens Res 6, 1994, 4, 53.
12. Cullity, B. D. Elements of X-Ray Diffraction; Addison-Wesley: Massachusetts, 1978; p 284.
13. Rong, H.; Leon, R.; Bhat, G. S. Text Res J 2005, 75, 35.
14. Nanjundappa, R.; Bhat, G. S.; Malkan, S. R. Proceedings of the INTC'2000, Sept. 2000.